

## The effect of microstructural heterogeneities on the fracture behaviour of three-directional carbon–carbon composites

H. AGLAN

Department of Mechanical Engineering, Tuskegee University, Tuskegee, AL 36088, USA

In very recent years the mechanical and thermal properties of carbonaceous materials have improved significantly due to the addition of reinforcing fibres in the matrix. Three-directional (3-D) carbon–carbon (C/C) composites represent one of the important types of C/C composites. This is due to the fact that their preform structure can be tailored in three directions, reflecting the final properties required of the material. The 3-D integrated preform structure of these composites results in superior damage tolerance and minimum delamination crack growth under interlaminar shearing compared with 2-D laminate C/C composites.

The preform structures of 3-D C/C composites are highly porous products and further densification cycles are required to achieve the final desired quality of the composites. The very nature of the densification techniques, coupled with the coarse orthotropic texture of yarn bundles and the anisotropy of the graphitic matrix induce severe microstructural heterogeneities. An important consequence of such anisotropy is the matrix voids and the microcracks introduced during manufacture. These microcracks can be formed both at the interface and within the yarn bundles, as shown in Fig. 1 [1]. In this letter the effect of microstructural heterogeneities on the fracture behaviour of 3-D C/C composites is considered. Efforts are made to study the fracture processes in view of the inherent microstructural complexity.

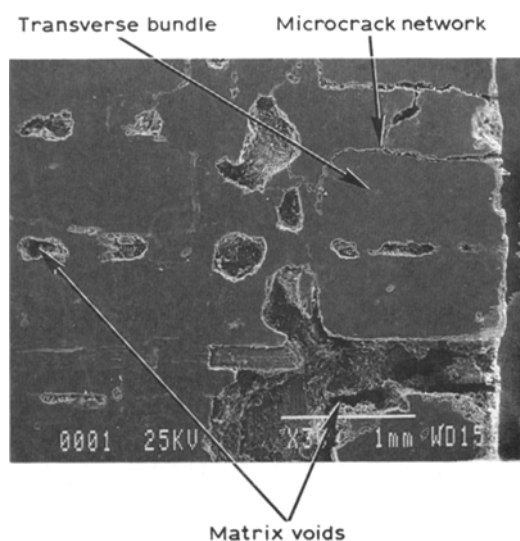


Figure 1 Photomicrograph of a polished cross-section, showing the microstructural heterogeneities of the 3-D C/C composite.

The material considered in the present work was a 3-D C/C composite manufactured in a disc form. The processing history of the billet includes seven impregnation–graphitization cycles with coal tar pitch. The average thickness of the billet was about 6.5 mm. Tests were conducted on three-point bend unnotched and notched specimens under monotonic loading. The specimen height and span were 14 and 48 mm, respectively. A 3 mm notch was introduced using a 0.38 mm thick milling cutter. The notch was cut in the radial direction of the disc, i.e. the crack was always initiated from the inside to the outside of the disc. The tests were conducted using displacement control with a crosshead speed of  $50 \mu\text{m min}^{-1}$ .

The load versus load-point displacement (LPD) curves were generated by continuously monitoring the load and crosshead displacement during testing. A clip gauge was used to monitor the crack-opening displacement (COD). The tip of the notch was viewed using a traveling optical microscope. A video system was attached to the microscope in order to obtain interval records of crack propagation and to record any damage events that could be observed. 14 macroscopically identical notched specimens were fractured under identical test conditions. Three unnotched specimens were also fractured under the same set of conditions. The loading behaviour, damage events and crack paths were observed in order to generate a database on the global fracture behaviour of this particular composite.

The average ultimate flexural strength based on the unnotched specimens was found to be 43 MPa. The flexural modulus was approximated using the formula from linear-elastic beam theory. It should be emphasized that only the first linear portion of the load versus LPD curve was used in the flexural modulus calculation. Any bimodular effects on the bending deflection were also ignored. The value of the flexural modulus,  $E_f$ , for the 3-D composite under investigation was found to be about 2.3 GPa. Although the value of  $E_f$  appears to be extremely low, this is not surprising. Similar values have been reported [2] for a C/C composite with a precursor felt material manufactured in a conical form. These values range from 2.75 to 10.3 GPa, depending on the loading direction. It has also been reported [3–5] that an increase in the number of graphitization cycles considerably decreases the elastic modulus. The material in the present investigation underwent seven impregnation–graphitization cycles.

Typical load versus LPD and load versus COD curves for a notched specimen of this composite are shown in Figs 2 and 3, respectively. Both curves exhibit the same trend. At the beginning there is a linear portion, followed by another of increased non-linearity. After a peak is reached major damage events take place, causing successive load drops as shown in Figs 2 and 3. Each load drop is preceded by an approximately constant load plateau. This type of behaviour represents steps of stable crack propagation and will be explored in more detail later.

Fracture toughness is traditionally characterized by the critical stress intensity factor  $K_{Ic}$  [6] for brittle materials complying with linear elasticity. On the other hand, the critical energy release rate  $J_{Ic}$  [7] is employed for ductile materials displaying elastic-plastic behaviour. However, the following relationship generally holds under plane strain conditions:

$$J_{Ic} = G_{Ic} = K_{Ic}^2 (1-\nu^2)/E$$

where  $E$  is Young's modulus and  $\nu$  is Poisson's ratio. On this basis the average value of  $G_{Ic}$  for the 3-D C/C composite under consideration is found to be  $4.6 \text{ kJ m}^{-2}$ , with the data ranging between  $2.7$  and  $7.4 \text{ kJ m}^{-2}$ . Due to the large (about three-fold) scatter in the data, a single value of  $G_{Ic}$  may not be sufficient to characterize this material fully.

Both the load versus LPD and the load versus COD curves display significant non-linearity as they approach their maximum where the onset of crack propagation takes place. This non-linear behaviour is indicative of dissipative activities before crack

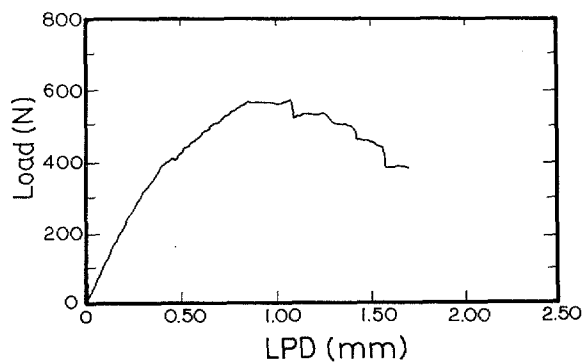


Figure 2 Load versus load point displacement (LPD) for one notched specimen of the 3-D C/C composite.

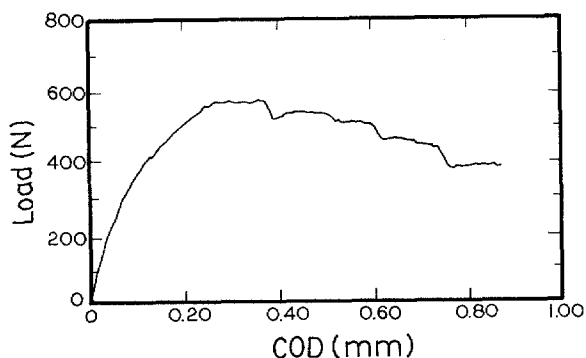


Figure 3 Load versus crack opening displacement (COD) for the same specimen shown in Fig. 2.

initiation. Heterogeneities are induced during processing (Fig. 1), which allow certain events to occur before crack initiation. These include coalescing, sliding and opening of the interfacial microcracks before fibre bundle failure. The very nature of these dissipative processes can render the characterization of 3-D C/C composites on the basis of linear-elastic fracture mechanics invalid. The microstructural heterogeneities also impart other undesirable attributes; that is, unpredictable and complex fracture behaviour. This casts further doubt on the usefulness of linear-elastic fracture mechanics for the characterization of these materials.

The current study was extended to examine the complex fracture processes. So far, a complete picture of the fracture processes of the 3-D C/C composites on both the macro- and micro-scales is not clear. It is believed that shear can occur at the crack tip [8, 9], which can remove the intensity of the stress at the crack tip [10], resulting in overall bundle failure rather than microscopic crack propagation. Extensive failure analysis is therefore required to elucidate this problem.

The failure of 3-D C/C composites can be better probed in view of the current experimental observations. In this work four of the notched specimens were polished and photographed before testing. Fig. 4 shows one such specimen before testing. A slow playback of the recorded video tape reveals that the crack initiated from the centre of the notch. It then advanced by a series of steps involving matrix and cross-bundle fracture processes. These steps correspond to the distinct load drops shown in both the load-deflection and the load-COD behaviour. A stable crack grew from the notch tip in the specimen (Fig. 4) and advanced to about 33% of the remaining unnotched ligament, corresponding to about four yarn bundles. This crack propagation immediately before the critical point was captured from the video screen and is shown in Fig. 5. The point of unstable crack propagation can be observed from the micrograph of half of the broken specimen shown in Fig. 6. At the point of unstable crack propagation the fracture path becomes less tortuous.

Thus, it appears that the failure of 3-D C/C composites involves a series of steps of stable crack propagation across both the matrix and the yarn bundles, followed by a catastrophic failure; unstable crack propagation. The failure of 3-D C/C composites appears to be dictated by the overall integrity of

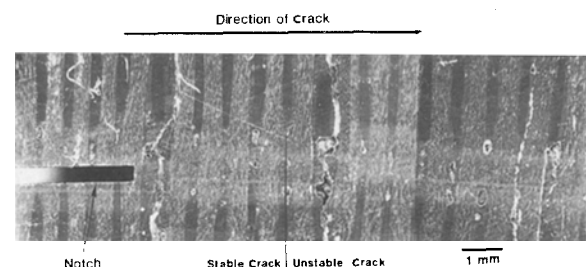


Figure 4 Photomicrograph of an unbroken specimen, showing details of both yarn bundles and the matrix ahead of the notch.

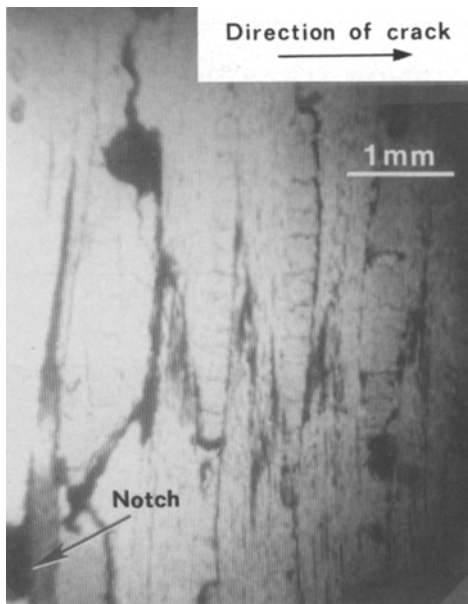


Figure 5 Photomicrograph of the propagating crack immediately before unstable crack propagation (taken from the video screen).



Figure 6 Photomicrograph of the bottom half of the fractured specimen of Fig. 5.

the preform structure. An applied load is not only acting on one or several bundles, it is acting on the whole structure. Again, the considerable stable crack propagation associated with the fracture of 3-D C/C composites casts more doubt on the validity of  $G_{Ic}$  as a material parameter characteristic of its resistance to crack propagation.

In summary, unlike in conventional materials, the

fracture toughness of 3-DC/C composites cannot be characterized by a single deterministic parameter. The strength fields of these composites appear to be random in nature. This is due to the coarse orthotropic texture of the yarn bundles, the anisotropy of the matrix and the microcrack network induced by thermal stress during processing. The fracture paths of 3-D C/C composites reflect the constraints imposed by the yarn bundles and the overall integrity of the preform structure. Unlike conventional materials, the crack in 3-D C/C composites diffuses in a tortuous manner, probably tracking pre-existing voids or microcracks. The failure of 3-D C/C composites involves a series of stable crack propagation steps across the matrix and yarn bundles, followed by unstable crack propagation. The dominant damage mechanisms associated with this type of failure are bundle breakage and matrix cracking.

## References

1. H. AGLAN and A. MOET, in "Design and manufacturing of advanced composites" (American Society for Metals International, Metals Park, Ohio, 1989) p. 83.
2. T. R. GUESS and W. R. HOOVER, *J. Compos. Mater.* **7** (1973) 2.
3. E. FITZER and A. GKOGKIDIS, in "Petroleum derived carbon", edited by J. Bacha, J. W. Newman and J. L. White, American Chemical Society Series No. 303 (ACS, Washington, DC, 1986) p. 346.
4. R. MEYER and S. GYETVAY, *ibid.* p. 380.
5. H. AGLAN, *SAMPE Int. Symp.* **36** (1991) 2237.
6. AMERICAN SOCIETY FOR TESTING AND MATERIALS ASTM Standard E399-81, Standard Test Methods for Plane Strain Fracture Toughness of Metallic Materials (1981).
7. AMERICAN SOCIETY FOR TESTING AND MATERIALS ASTM Standard E813-81, Standard Test for  $J_{Ic}$ ; A Measure of Fracture Toughness (1981).
8. A. KELLY, *Proc. R. Soc.* **A319** (1970) 95.
9. P. BEAMONT and D. PHILLIPS, *J. Compos. Mater.* **6** (1972) 32.
10. D. PHILLIPS, *ibid.* **8** (1974) 130.

Received 4 July 1990

and accepted 8 May 1991